Surface Characterization of La_2O_3−TiO_2 and V_2O_5/La_2O_3−TiO_2 Catalysts

Benjaram M. Reddy,*,† Pavani M. Sreekanth, and Ettireddy P. Reddy

Inorganic and Physical Chemistry Division, Indian Institute of Chemical Technology, Hyderabad - 500 007, India

Yusuke Yamada, Qiang Xu, Hiroaki Sakurai, and Tetsuhiko Kobayashi*,‡

National Institute of Advanced Industrial Science and Technology (AIST), 1-8-31 Midorigaoka, Ikeda, Osaka, 563-8577, Japan

Received: December 10, 2001; In Final Form: March 20, 2002

The techniques of X-ray diffraction, O_2 chemisorption, FT-Raman, and X-ray photoelectron spectroscopy were utilized to characterize La_2O_3−TiO_2 composite oxide and V_2O_5/La_2O_3−TiO_2 catalyst calcined at 773 and 1073 K temperatures. The investigated La_2O_3−TiO_2 (1:5 mole ratio) mixed oxide was obtained by a homogeneous coprecipitation method with in situ generated ammonium hydroxide. A nominal 12 wt % V_2O_5 was impregnated over the calcined (773 K) composite oxide by adopting a wet impregnation method from ammonium metavanadate dissolved in aqueous oxalic acid solution. The characterization results suggest that the calcined La_2O_3−TiO_2 mixed oxide primarily consists of a mixture of TiO_2 anatase and La−Ti oxides. The La_2O_3−TiO_2 also accommodates a monolayer equivalent of vanadia in a highly dispersed state. The O 1s, Ti 2p, La 3d, and V 2p photoelectron peaks of the V_2O_5/La_2O_3−TiO_2 sample are highly sensitive to the calcination temperature. The XPS line shapes and the corresponding binding energies indicate that the dispersed vanadium oxide interacts selectively with the lanthana portion of the La_2O_3−TiO_2 mixed oxide and readily forms a $LaVO_4$ compound. The XRD and FT-Raman techniques, in particular, provide direct evidence for the formation of $LaVO_4$ compound. Interestingly, the presence of lanthana in V_2O_5/La_2O_3−TiO_2 catalysts retards the phase transformation of anatase into rutile under the influence of vanadia.

Introduction

Supported vanadium oxide catalysts have been investigated quite extensively because of their technological importance in several industrial heterogeneous catalytic processes, such as partial oxidation or oxidative dehydrogenation of various hydrocarbons, ammoxidation of aromatic compounds, and selective catalytic reduction (SCR) of nitrogen oxides.[1−15] As a consequence, considerable attention has been devoted to the characterization of vanadium oxide species on various supports.[1,2,4,5,10,16−24] Most of these studies reveal that the activity and selectivity of supported vanadium oxide catalyst is very sensitive to the nature of support and in the case of TiO_2-supported catalysts, the phase of support. Earlier investigations further disclosed that the preferred phase of TiO_2 is anatase and that the activity per gram of catalyst increases with increase of vanadium oxide loading up to the point where the surface of the support is covered by a theoretical monolayer of V_2O_5. The stronger redox characteristics of the TiO_2 is yet another important factor for the dramatic promotional effect of titania support on the catalytic performance of surface vanadium oxide species.[24] However, a major disadvantage associated with TiO_2 support is its relatively low specific surface area and low thermal stability of the active anatase structure at high temperatures.[9] Increasing the lifetime of catalysts for SCR of NO_x and for removal of volatile organic compounds (VOCs) is one of the biggest challenges of the catalyst development studies today. Sintering of TiO_2 may result from several processes, one of which is phase transformation from anatase into the thermodynamically stable rutile form. Since the transformation of the metastable anatase phase is irreversible, loss of activity is a permanent phenomenon. Therefore, titania was combined with other stable oxides such as alumina or silica to stabilize the surface area and the structure of anatase.[16,17,25−33]

Lanthanum oxide is one of the best stabilizers for inhibiting the sintering of high surface area γ-alumina.[34,35] The La_2O_3 is particularly adopted for the reactive atmosphere that contains water.[36] The La_2O_3−TiO_2 composite material is also employed for various purposes in the literature, such as oxidation of chlorodifluoromethane,[37] oxidative coupling of methane,[38,39] automobile catalytic converter, ceramic membrane top layer, and adsorbent.[40,41] The La_2O_3 incorporated TiO_2 mixed oxide, after impregnating with vanadium oxide, was found to exhibit excellent catalytic performance for one -step synthesis of 2,6-dimethylphenol from methanol and cyclohexanone mixtures.[42] The 2,6-dimethylphenol is an important chemical intermediate in the polymer industry for engineering plastics. The V_2O_5/La_2O_3−TiO_2 mixed oxide catalyst possesses a combination of acid−base and redox characteristics together, thus, exhibits very interesting catalytic properties. In view of its significance, a comprehensive investigation was undertaken by the authors to fully understand the evolution and physicochemical characteristics of this complex catalyst system.

The aim of the present investigation, in particular, was to provide basic insights into the structure of La_2O_3−TiO_2 support and V_2O_5/La_2O_3−TiO_2 catalyst under the influence of thermal

* Corresponding authors.
† Fax: +91-40-716-0387. E-mail: bmreddy@iict.ap.nic.in.
‡ Fax: +81-727-51-9630. E-mail: t-kobayashi@aist.go.jp.

10.1021/jp014487p CCC: $22.00
Published on Web 05/14/2002

treatments. In this study, a $La_2O_3-TiO_2$ (1:5 mole ratio) composite oxide was prepared by a homogeneous coprecipitation method with in situ generated ammonium hydroxide and was impregnated with a nominal 12 wt % V_2O_5. The prepared samples were calcined at 773 and 1073 K in order to understand the temperature stability and physicochemical properties of these materials. Characterization techniques such as XRD, BET surface area, O_2 chemisorption, FT-Raman, and XPS were used to monitor the influence of thermal effects on these materials.

Experimental Section

Catalyst Preparation. The $La_2O_3-TiO_2$ composite oxide (1:5 mole ratio based on oxides) was prepared by an aqueous homogeneous coprecipitation method where ammonium hydroxide was generated in situ by decomposition of urea at 368 K.[43] For precipitation with urea, a mixed aqueous solution of $TiCl_4$ (Fluka, AR grade), $La(NO_3)_3 \cdot 6H_2O$ (Loba Chemie, GR grade), and urea (Loba Chemie, GR grade) was heated to 368 K with vigorous stirring. To make the above mixed aqueous solution, $TiCl_4$ that was first digested in cold concentrated HCl and subsequently diluted with doubly distilled water and then $La(NO_3)_3$, dissolved separately in doubly distilled water, was added (pH = 2). An excess amount of solid urea with a metal-to-urea mole ratio of 1:1.5 was also added to this mixture in solution. In about 6 h of heating, as decomposition of urea progressed to a certain extent, the formation of precipitate gradually occurred and the pH of the solution increased to 7−8. Heating was continued at this temperature for 6 h more and the pH of the solution increased to 8−9 by adding dilute ammonia in order to complete the precipitation and to facilitate aging. The resulting precipitate was then filtered off, washed several times with deionized water until free from chloride ions, and dried at 393 K for 16 h. The oven-dried material was finally calcined at 773 K for 6 h in air atmosphere. Some portions of this finished $La_2O_3-TiO_2$ sample were once again heated at 1073 K in a closed electrical furnace in an air atmosphere.

The $V_2O_5/La_2O_3-TiO_2$ catalyst containing 12 wt % V_2O_5 was prepared by a standard wet-impregnation method. To obtain the supported vanadia, the required quantity of ammonium metavanadate (Fluka, AR grade) was dissolved in 1 M aqueous oxalic acid, and the finely powdered calcined $La_2O_3-TiO_2$ support was added to this solution. The excess water was evaporated on a water bath with continuous stirring. The resulting sample was oven dried at 383 K for 12 h and calcined at 773 K for 5 h in a closed electrical furnace in a flowing oxygen atmosphere. Some portions of this finished catalyst were once again heated at 1073 K for 5 h in a closed electrical furnace in an air atmosphere.

Catalyst Characterization. X-ray powder diffraction patterns have been recorded on a Rigaku RINT 2000 instrument, using Cu Kα radiation and standard recording conditions. The XRD phases present in the samples were identified with the help of JCPDS data files. The specific surface area of the samples was determined on a conventional standard static volumetric high vacuum (1×10^{-4} Pa) system by N_2 physisorption at liquid N_2 temperature and by taking 0.162 nm^2 as the molecular area of N_2 molecule. Before the measurements, the samples were dried in situ at 473 K for 2 h under vacuum. The same standard volumetric high-vacuum system, with the facility for reducing the sample in situ by flowing purified hydrogen (35 $cm^3\ min^{-1}$), was used for oxygen uptake measurements. The catalyst sample (ca. 0.5 g) was reduced for 4 h at 643 K followed by evacuation at the same temperature for 2 h (1×10^{-4} Pa) prior to O_2 uptake. The amount of O_2 chemisorbed was then determined as the difference between two successive adsorption isotherms obtained at 643 K. Keeping the adsorption temperature constant (643 K), the sample was evacuated for 1 h between the first and second adsorptions. More details of this method can be found elsewhere.[44] Raman spectra were recorded at ambient temperature on a Nicolet FT-Raman 960 Spectrometer with a range of 4000−100 cm^{-1} and a spectral resolution of 2 cm^{-1} using the 1064 nm exciting line (~600 mV) of a Nd:YAG laser (Spectra Physics, USA). Finely powdered samples were contained in a 5 mm o.d. NMR tube. Before measurements, samples were dried in a vacuum oven for several hours. The XPS measurements were made on a Shimadzu (ESCA 3400) spectrometer by using Mg Kα (1253.6 eV) radiation as the excitation source. Charging of catalyst samples was corrected by setting the binding energy (BE) of adventitious carbon (C 1s) line at 284.6 eV.[45,46] The finely ground oven-dried samples were dusted on a double stick graphite sheet and mounted on the standard sample holder. The sample holder was transferred to the analysis chamber, which can house 10 samples at a time, through a rod attached to it. The XPS analysis was done at room temperature and pressures were typically in the order of less than 10^{-6} Pa. The samples were outgassed in a vacuum oven overnight before XPS measurements.

TABLE 1: The N_2 BET Surface Area and O_2 Chemisorption Capacities of $La_2O_3-TiO_2$ and 12 wt % $V_2O_5/La_2O_3-TiO_2$ Samples

sample	calcination temp. (K)	BET SA ($m^2\ g^{-1}$ cat.)	O_2 uptake (μmol g^{-1}-cat.)	% dispersion (O/V)
$La_2O_3-TiO_2$	773	123	5.2	
$La_2O_3-TiO_2$	1073	38	2.8	
$V_2O_5/La_2O_3-TiO_2$	773	63	256	39
$V_2O_5/La_2O_3-TiO_2$	1073	12	48	10

Results and Discussion

The BET surface areas of $La_2O_3-TiO_2$ and 12% $V_2O_5/La_2O_3-TiO_2$ samples calcined at different temperatures are presented in Table 1. The $La_2O_3-TiO_2$ support calcined at 773 K exhibited a N_2 BET surface area of 123 $m^2\ g^{-1}$. The theoretical quantity of vanadia required to cover the support surface as a thin monolayer can be estimated from the area occupied per $VO_{2.5}$ unit of the bulk V_2O_5 (0.105 nm^2).[8] The theoretical estimation yields a loading of 0.145 wt %/m^2 of the support to cover its surface with a compact single lamella of vanadium pentoxide structure.[4] However, the maximum amount of vanadium oxide that can be formed as a thin two-dimensional monolayer depends not only on the support specific surface area but also on the concentration of reactive surface hydroxyl groups. Therefore, the experimentally determined actual loading was always less than the theoretical estimation and corresponds to about 70% of the theoretical value.[4] In view of these reasons, a 12 wt % V_2O_5 loading was selected in the present investigation to impregnate on the $La_2O_3-TiO_2$ support. As can be noted from Table 1, the BET surface of the $La_2O_3-TiO_2$ was found to decrease from 123 to 63 $m^2\ g^{-1}$ after impregnating with vanadium oxide and calcined at 773 K. The decrease in the specific surface area of the support after impregnating with V_2O_5 is a general phenomenon observed on various oxide supports.[4,5,29,33,44,47] This is primarily due to the penetration of the dispersed vanadium oxide into the pores of the support, thereby narrowing its pore diameter and blocking some of the micropores. The solid-state reactions between the dispersed vanadium oxide and the support may also contribute to the observed decrease in the surface areas of the samples. A further

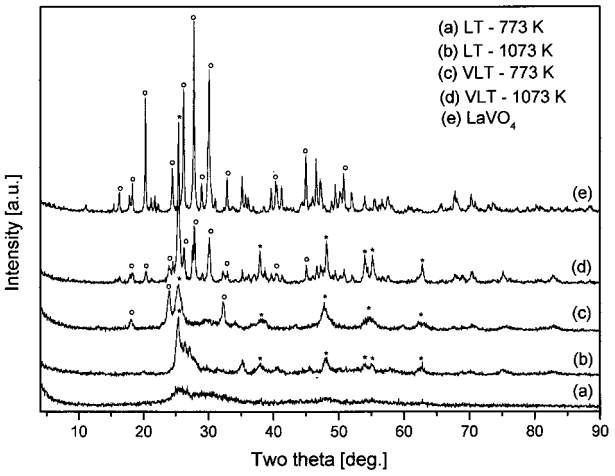

Figure 1. X-ray powder diffraction patterns of $La_2O_3-TiO_2$ (LT) and 12% $V_2O_5/La_2O_3-TiO_2$ (VLT) samples calcined at different temperatures. For comparison, the XRD pattern of $LaVO_4$ is also shown in this figure: (*) lines due to anatase; (*o*) lines due to $LaVO_4$.

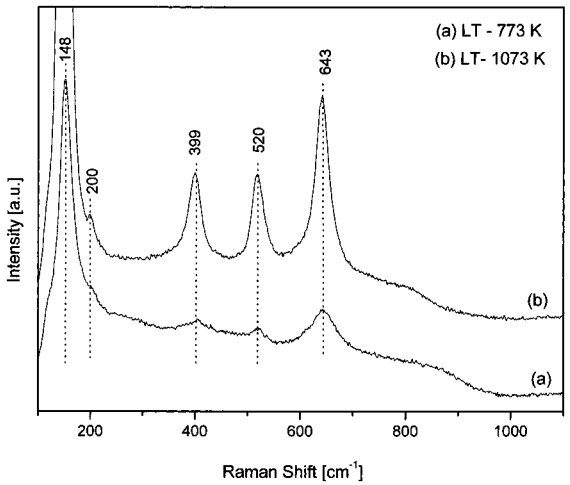

Figure 2. FT-Raman spectra of $La_2O_3-TiO_2$ (LT) sample calcined at different temperatures.

decrease in the surface area of the $La_2O_3-TiO_2$ support and the $V_2O_5/La_2O_3-TiO_2$ catalyst, after subjecting them to 1073 K, is due to sintering of the samples at higher calcination temperatures. An important point to be noted from Table 1 is that the decrease in the specific surface area is more in the case of vanadium oxide impregnated samples than that of pure support. In other words, the pure lanthana−titania support is more thermally stable when compared to that of vanadium oxide impregnated samples. The O_2 uptake capacity of the $V_2O_5/La_2O_3-TiO_2$ sample and the dispersion of vanadium oxide on the support as a function of temperature are shown in Table 1. The dispersion, defined as the ratio of molecular oxygen uptake to V_2O_5 content, can be determined from O_2 uptake measurements.[18,22,44] The technique of O_2 chemisorption has been widely employed to determine the dispersion of vanadium oxide on various supports since O_2 uptake is possible only on the reduced V oxide, which contains the coordinately unsaturated sites.[4,18,22,29,47] This method discriminates between the dispersed monolayer and the crystalline V oxide phase since their reduction behaviors are entirely different. The O_2 uptake capacity of the $V_2O_5/La_2O_3-TiO_2$ sample (773 K) was found to be relatively less when compared to that of other catalyst systems such as V_2O_5/TiO_2-SiO_2, $V_2O_5/TiO_2-Al_2O_3$, and V_2O_5/TiO_2-ZrO_2 reported earlier.[22,29,47] This could be due to a strong interaction between the dispersed vanadium oxide and lanthanum oxide leading to the formation of $LaVO_4$ compound, thereby decreasing the amount of the dispersed V oxide on the surface of the support. This observation has been confirmed from XRD, FT-Raman measurements as described in the following paragraphs. In the case of the 1073 K calcined sample, the decrease in the dispersion with increase in calcination (Table 1) temperature is primarily due to sintering of the sample.

The XRD patterns of the $La_2O_3-TiO_2$ support and the $V_2O_5/La_2O_3-TiO_2$ catalyst calcined at 773 and 1073 K are shown in Figure 1. As can be noted from this figure, the $La_2O_3-TiO_2$ binary oxide support prepared via a homogeneous coprecipitation method and calcined at 773 K is in X-ray amorphous state with broad background diffraction lines due to TiO_2 anatase phase (JCPDS File No. 21-1272). With an increase of calcination temperature from 773 to 1073 K an improvement in the intensity of the lines due to TiO_2 anatase can be observed. In addition to the TiO_2 anatase lines, a few other undefined lines were also noted, which could be due to the formation of $La_2Ti_2O_7$ and $La_4Ti_9O_{24}$ compounds whose presence was reported by Gopalan and Lin, recently.[48] They reported the formation of $La_2Ti_2O_7$ at 973 K, and $La_4Ti_9O_{24}$ at 1073 K and above temperatures in a sample having the appropriate composition of titania and lanthana components and prepared by adopting a different method. Most importantly, no X-ray powder diffraction lines due to TiO_2 rutile phase (JCPDS File No. 21-1276) are observed in the present study. In the case of the $V_2O_5/La_2O_3-TiO_2$ sample, a few notable changes could be seen. At 773 K calcination, an improvement in the intensity of the anatase lines can be noted. This is primarily due to the influence of dispersed vanadia on the crystallization of TiO_2. It is an established fact in the literature that the dispersed vanadia on titania support enhances the crystallization of TiO_2 and its subsequent phase transformation from anatase into rutile.[4,8,43] In addition to the strong TiO_2 anatase lines, a few broad diffraction lines due to $LaVO_4$ (JCPDS File No. 25-0427) compound can also be noted from Figure 1. On increase of calcination temperature from 773 to 1073 K an improvement in the intensity of the lines due to anatase and $LaVO_4$ can be noted. There are also a few other undefined lines due to La−Ti oxides, as observed in the case of pure support, whose intensity was also found to increase. Most importantly, no XRD lines due to TiO_2 rutile phase are noted. A total anatase-to-rutile phase transformation is normally expected at 1073 K in the case of V_2O_5/TiO_2 catalyst containing even lesser amounts of V_2O_5.[4,49] However, in the present study the observation of anatase lines even after calcination at 1073 K in a sample containing 12 wt % V_2O_5 gives an impression that the lanthanum oxide added to the titania support retards the phase transformation of anatase into rutile. This is an interesting observation from the present study. Retaining the TiO_2 anatase beyond 1073 K is highly useful for application of these composite oxides for various purposes as outlined in the Introduction. To confirm the formation of $LaVO_4$ compound, the XRD patterns of the same is also shown in Figure 1. As can be noted from this figure, the formation of $LaVO_4$ can be established beyond doubt in the case of the $V_2O_5/La_2O_3-TiO_2$ sample calcined at 1073 K. In the XRD patterns of $LaVO_4$ (trace, e), a few unassigned very weak reflections could be seen which are primarily due to the presence of undecomposed precursors.

The Raman spectra of the $La_2O_3-TiO_2$ support and the 12% $V_2O_5/La_2O_3-TiO_2$ catalyst calcined at two different temperatures are shown in Figures 2 and 3, respectively. As per the literature, the anatase phase of TiO_2 possesses Raman features at 144, 199, 399, 520, and 643 cm^{-1} and the rutile phase at

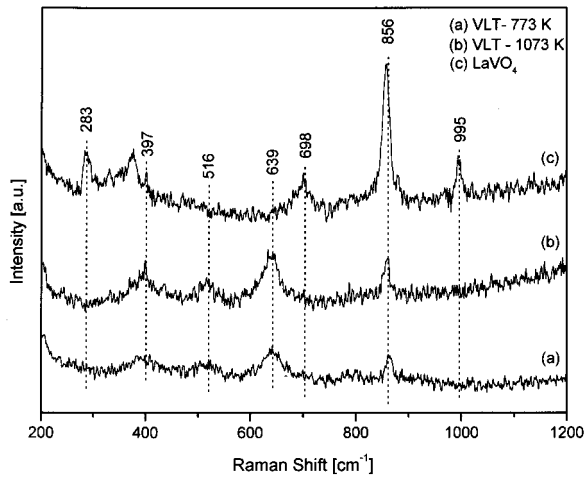

Figure 3. FT-Raman spectra of 12% $V_2O_5/La_2O_3-TiO_2$ (VLT) sample calcined at different temperatures. For comparison, the FT-Raman spectrum of $LaVO_4$ is also shown in this figure.

144, 148, and 611 cm^{-1}, respectively.[50,51] As can be noted from Figure 2, the $La_2O_3-TiO_2$ sample calcined at 773 K shows all characteristic Raman bands due to TiO_2 anatase. On increase of calcination temperature from 773 to 1073 K, an increase in the intensity of the Raman bands due to anatase phase can be noted. No characteristic bands due to TiO_2 rutile or La_2O_3 or La−Ti oxides can be observed. In the case of $V_2O_5/La_2O_3-TiO_2$ sample (Figure 3), in addition to all characteristic anatase bands, a strong band at 856 cm^{-1} and few very weak bands at around 698, 397, and 1002 cm^{-1} can be noticed. The Raman spectrum of $LaVO_4$ is also shown in Figure 3 for the purpose of comparison. As can be noted from Figure 3, there is clear evidence for the formation of $LaVO_4$ in the case of $V_2O_5/La_2O_3-TiO_2$ sample. As reported in the literature, the tetrahedral VO_4^{3-}, as present in aqueous solution, has the most prominent Raman band at 827 cm^{-1} and for solids, with isolated VO_4^{3-} units, this band lies in the range 830−855 cm^{-1}.[52] This band is associated with symmetric stretching mode of the metal−oxygen bonds (−O−V−O−). In accordance with the literature, the Raman bands of the supported metal oxide catalysts in the range between 1050 and 950 cm^{-1} can be assigned to the stretching mode of the short terminal M═O bonds, whereas the bands in the range between 950 and 750 cm^{-1} are attributed to either the anti-symmetric stretch of M−O−M bonds or the symmetric stretch of $(-O-M-O-)_n$ bonds.[53,54] The major peak of crystalline V_2O_5 assigned to the V═O stretching mode appears at 995 cm^{-1}. Due to a relatively large Raman scattering cross section of V_2O_5 as compared to the cross section for supported vanadia species, Raman spectra of supported vanadia catalysts can appear to be essentially similar to the bulk V_2O_5.[4] As can be noted from Figure 3, no Raman bands duo to crystalline or dispersed vanadia phase can be observed. As observed from XRD measurements, the $V_2O_5/La_2O_3-TiO_2$ sample contains various components such as TiO_2 anatase, $LaVO_4$, and undefined La−Ti oxides. The Raman measurements clearly support the observations made from XRD study.

The samples of $La_2O_3-TiO_2$ and $V_2O_5/La_2O_3-TiO_2$ calcined at two different temperatures have been investigated by XPS technique. The photoelectron peaks of O 1s, La 3d, and V 2p pertaining to these samples are shown in Figures 4−6, respectively, and the corresponding electron binding energies (E_b) and the full width at half-maximum (fwhm) values are shown in Table 2. As can be noted from these figures and Table 2 that the photoelectron peaks of these samples are highly sensitive to the calcination temperature and the coverage of vanadium

TABLE 2: Electron Binding Energies (eV) and fwhm (eV) Values for $La_2O_3-TiO_2$ and 12 wt % $V_2O_5/La_2O_3-TiO_2$ Samples Calcined at Different Temperatures

		O 1s		Ti $2p_{3/2}$			V $2p_{3/2}$[a]	
sample	temp (K)	BE	fwhm	BE	fwhm	La $3d_{5/2}$	BE	fwhm
$La_2O_3-TiO_2$	773	530.1	1.74	458.6	1.68	834.9		
$La_2O_3-TiO_2$	1073	530.2	2.10	458.6	1.74	834.9		
$V_2O_5/La_2O_3-TiO_2$	773	530.7	2.45	458.9	1.95	835.4	515.9	2.85
$V_2O_5/La_2O_3-TiO_2$	1073	530.6	2.71	458.8	2.33	835.2	516.0	3.37

[a] The BE values for the main peak as shown in Figure 6A. However, it is composed of three peaks with different binding energies corresponding to various oxidation states, shown in Figure 6B and elaborated in the text.

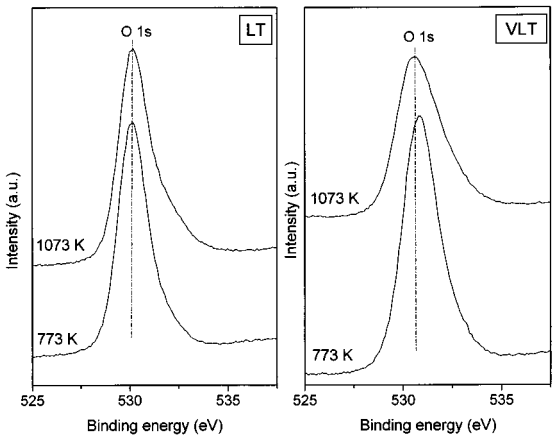

Figure 4. The O 1s XPS spectra of $La_2O_3-TiO_2$ (LT) and $V_2O_5/La_2O_3-TiO_2$ (VLT) samples calcined at different temperatures.

oxide on the $La_2O_3-TiO_2$ composite oxide. As presented in Figure 4, the O 1s profile is, in general, more complicated due to the overlapping contribution of oxygen from lanthana and titania in the case of $La_2O_3-TiO_2$ support and from lanthana, titania, and vanadia in the case of the $V_2O_5/La_2O_3-TiO_2$ sample. Mainly, two distinct oxygen peaks are observed for the $La_2O_3-TiO_2$ support as well as for the $V_2O_5/La_2O_3-TiO_2$ sample calcined at two different temperatures. In the case of pure support, it can be easily assigned that the intense peak at lower binding energy (E_b = 530.1 eV) is due to the oxygen atoms that are bound to Ti (i.e., TiO_2) and the one at higher binding energy (E_b = 530.6 eV) belonging mainly to La, judging from the difference in the electronegativity of the elements involved and from literature.[45,46,55] In the case of pure support, the binding energies of the O 1s peaks are almost constant with increase of calcination temperature. However, a slight increase in the binding energies and the fwhm values are observed in the case of vanadia-impregnated samples. This may be due to the selective interaction of the dispersed vanadium oxide with the lanthana portion of the $La_2O_3-TiO_2$ mixed oxide to form $LaVO_4$ compound and the crystallization of TiO_2 under the influence of vanadia as observed from XRD analysis. The maximum contributor for O 1s in $La_2O_3-TiO_2$ and $V_2O_5/La_2O_3-TiO_2$ samples is TiO_2 since its concentration is higher than that of other constituents.

As shown in Table 2, the binding energy of the Ti $2p_{3/2}$ photoelectron peak ranged between 458.6 and 458.9 eV, which agree well with values reported in the literature.[33,45,46] The intensity of the Ti 2p core level spectra was found to decrease slightly with increasing calcination temperature due to broadening. As presented in Table 2, broadening of the Ti 2p peak, in line with the O 1s peak, was also noted in the case of $V_2O_5/La_2O_3-TiO_2$ sample calcined at 1073 K. The broadening of the Ti 2p peak is mainly due to redistribution of various

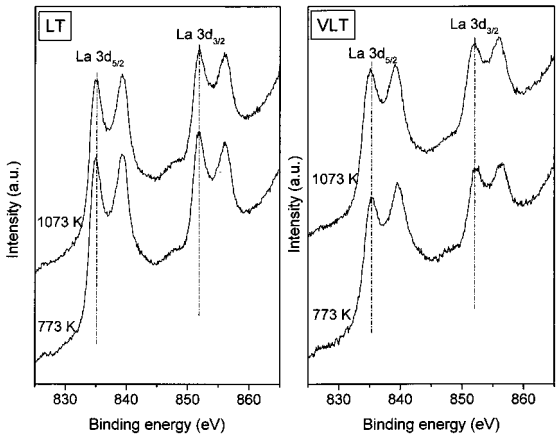

Figure 5. The La 3d XPS spectra of XPS spectra of $La_2O_3-TiO_2$ (LT) and $V_2O_5/La_2O_3-TiO_2$ (VLT) samples calcined at different temperatures.

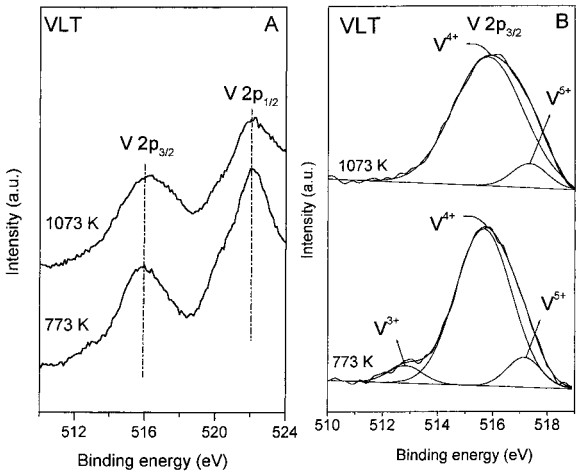

Figure 6. (A) The V 2p XPS spectra of $V_2O_5/La_2O_3-TiO_2$ (VLT) sample calcined at different temperatures. (B) The XPS deconvolution of V 2p peaks for $V_2O_5/La_2O_3-TiO_2$ (VLT) sample calcined at different temperatures.

components in the $V_2O_5/La_2O_3-TiO_2$ sample under the influence of high-temperature calcination. A total redistribution of various components is expected in the case of $V_2O_5/La_2O_3-TiO_2$ sample due to strong interaction between the acidic V_2O_5 and the basic La_2O_3 to form the stable $LaVO_4$ compound.

Figure 5 shows the binding energies of the La 3d photoelectron peaks at 834.9 and 851.8 eV for La $3d_{5/2}$ and La $3d_{3/2}$ lines, respectively, which agree well with the spectra reported in the literature.[45] In the case of $La_2O_3-TiO_2$ support, the intensity and binding energy of the La 3d line were observed to be same irrespective of calcination temperature. This indicates that the chemical state of lanthanum is the same in the support, irrespective of calcination temperature. However, in the case of $V_2O_5/La_2O_3-TiO_2$ catalyst, a slight increase in the binding energy (Table 2) can be noted. A slight increase in the intensity of the 3d peak with increasing calcination temperature can also be noted. The increase in the electron binding energy and the intensity changes are primarily due the formation of $LaVO_4$ compound as mentioned earlier. The XPS results thus synchronize with the observations made from XRD and FT-Raman measurements.

Figure 6 (a) shows the V 2p photoelectron peaks of the $V_2O_5/La_2O_3-TiO_2$ sample calcined at two different temperatures. The corresponding deconvolution of the V $2p_{3/2}$ peak is also shown in this Figure (b). The Figure 6(a) and the fwhm values shown in Table 2 indicate broadening of the V 2p line with increasing calcination temperature. Generally, the broadening of XPS peaks can be attributed to various factors including (1) the presence of more than one type of V^{5+} or V^{4+} species with different chemical characteristics, which cannot be discerned by ESCA, and (2) the electron transfer between the active component and the support (metal oxide−support interaction).[56] The deconvolution of the V $2p_{3/2}$ peak (Figure 6(b)) clearly indicates that there are at least three peaks (E_b = 513.1, 515.7, and 517.1 eV) and two peaks (E_b = 516.0 and 517.4 eV) for 773 and 1073 K calcined samples, respectively. A careful examination of the literature reveals that the V $2p_{3/2}$ binding energy reported for V_2O_5 (V^{5+} oxidation state) ranges between 516.4 and 517.4 eV; the next oxidation state, V^{4+}, represented by V_2O_4, shows values in the range of 515.4−515.7 eV.[4,57] Similarly, the E_b values reported for the lower oxidation state vanadium (V^{2+} and V^{3+}) in V-containing organometallic complexes ranged between 512.8 and 513.2 eV.[45,58,59] As can be envisaged from Figure 6(b) that the sample calcined at 773 K primarily consists of a mixture of $LaVO_4$ compound (probably V^{4+} species) and a highly dispersed V oxide phase (mostly in V^{5+} state) on the surface of the support. There is also a small presence of V^{3+} impurity species in the form of an organometallic complex. An aqueous oxalic acid solution was used to dissolve the ammonium metavanadate during the preparation of the catalysts. Therefore, it is quite possible to have some undecomposed lower oxidation state vanadium complex even after calcination at 773 K. However, its presence was not noticed in the case of the 1073 K calcined sample.

It is an established fact in the literature that the dispersed vanadium oxide on titania support accelerates the phase transformation of anatase to rutile. It is also known that during this phase transformation some of the dispersed vanadia is normally reduced and gets incorporated into the rutile structure as $V_xTi_{(1-x)}O_2$ (rutile solid solution).[4,8] However, the present investigation gives an impression that the dispersed vanadium oxide interacts preferentially with the lanthana instead of titania in the mixed oxide matrix. This strong interaction between the vanadia and the lanthana leads to the formation of a definite $LaVO_4$ compound as observed from XRD and FT-Raman measurements. Nevertheless, the composite $V_2O_5/La_2O_3-TiO_2$ mixed oxide catalyst exhibits very interesting catalytic properties.[42]

Conclusions

The following conclusions can be drawn from this study: (1) The $La_2O_3-TiO_2$ composite oxide obtained by a homogeneous coprecipitation method with in situ generated ammonium hydroxide exhibits reasonably high specific surface area and high thermal stability up to 1073 K calcination temperature. It primarily consists of a mixture of TiO_2 anatase and La−Ti oxides. (2) The lanthana−titania composite oxide is an interesting and promising support for the dispersion of vanadium oxide. Characterization of $V_2O_5/La_2O_3-TiO_2$ catalysts by XRD, FT-Raman, O_2 chemisorption, and XPS measurements reveal that the $La_2O_3-TiO_2$ mixed oxide also accommodates vanadium oxide (12 wt % V_2O_5) in a highly dispersed state. Presence of no crystalline V_2O_5 was observed from XRD and FT-Raman techniques. The dispersed vanadium oxide selectively interacts with the La_2O_3 portion of the $La_2O_3-TiO_2$ composite oxide and readily forms $LaVO_4$ compound. The $LaVO_4$ compound formation and the crystallization of TiO_2 anatase are sensitive to the calcination temperature. (3) In particular, the lanthana in $V_2O_5/La_2O_3-TiO_2$ catalysts retards the phase transformation of

anatase to rutile under the influence of vanadia. Finally, further studies are required in order to understand the microscopic mechanism of the solid-state reactions between the dispersed vanadium oxide and the lanthanum oxide.

Acknowledgment. B.M.R. acknowledges a senior STA visiting fellowship from the Japan Science and Technology Corporation (JST). We are grateful to Dr. A. Ueda and Dr. H. Ando for useful discussions.

References and Notes

(1) Vedrine, J. C., Ed. Eurocat Oxide. *Catal. Today* **1994**, *20*, 1 and references therein.
(2) Gellings, P. J. In *Catalysis*; Bond, G. C., Webb, G., Eds.; The Royal Society of Chemistry: London, 1985; Vol. 7, p 105.
(3) Nikolov, V.; Klissurski, D.; Anastasov, A. *Catal. Rev. Sci. Eng*. **1991**, *33*, 1.
(4) Bond, G. C.; Tahir, S. F. *Appl. Catal*. **1991**, *71*, 1 and references therein.
(5) Deo, G.; Wachs, I. E.; Haber, J. *Crit. Rev. Surf. Chem*. **1994**, *4*, 141.
(6) Albonetti, A.; Cavani, F.; Trifiro, F. *Catal. Rev. Sci. Eng*. **1996**, *38*, 413.
(7) Bosch, H.; Janssen, F. *Catal. Today* **1988**, *2*, 369.
(8) Roozeboom, F.; Mittelmeijer-Hazeleger, M. C.; Moulijin, J. A.; Medema, J.; de Beer, V. H.; Gellings, P. J. *J. Phys. Chem*. **1980**, *84*, 2783.
(9) Hadjiivnov, K.; Klissurski, D. G. *Chem. Soc. Rev.* **1996**, *25*, 61.
(10) Reddy, B. M.; Reddy, E. P.; Srinivas, S. T.; Mastikin, V. M.; Nosov, A. V.; Lapina, O. B. *J. Phys. Chem*. **1992**, *96*, 7076.
(11) Corma, A.: López Nieto, J. M.; Paredes, N. *Appl. Catal A: General* **1993**, *97*, 159.
(12) Eon, J. G.; Oliver, R.; Volta, J. C. *J. Catal*. **1994**, *145*, 318.
(13) Kung, H. H.; Kung, M. C. *Appl. Catal. A: General* **1997**, *157*, 105.
(14) Khodakov, A.; Olthof, B.; Bell, A. T.; Iglesia, E. *J. Catal*. **1999**, *181*, 205.
(15) Zhao, Z.; Yamada, Y.; Teng, Y.; Ueda, A.; Nakagawa, K.; Kobayashi, T. *J. Catal*. **2000**, *190*, 215.
(16) Concepción, P.; Reddy, B. M.; Knözinger, H. *Phys. Chem. Chem. Phys*. **1999**, *1*, 3031.
(17) Baiker, A.; Dollenmeier, P.; Glinski, M.; Reller, A. *Appl. Catal*. **1997**, *35*, 351.
(18) Oyama, S. T.; Went, G. T.; Lewis, K. B.; Bell, A. T.; Somorjai, G. A. *J. Phys. Chem*. **1989**, *93*, 6786.
(19) Patil, D.; Anderson, P. J.; Kung, H. H. *J. Catal*. **1990**, *125*, 132.
(20) Khodakov, A.; Yang, J.; Su, S.; Iglesia, E.; Bell, A. T. *J. Catal*. **1998**, *177*, 343.
(21) Adamski, A.; Sojka, Z.; Dyrek, K.; Che, M.; Wendt, G.; Albrecht, S. *Langmuir* **1999**, *15*, 5733.
(22) Reddy, B. M.; Chowdhury, B.; Reddy, E. P.; Fernández, A. *Langmuir* **2001**, *17*, 1132.
(23) Vejux, A.; Courtine, P. *J. Solid State Chem*. **1978**, *23*, 93.
(24) Deo, G.; Wachs, I. E. *J. Catal*. **1991**, *129*, 307.
(25) Rajadhyaksha, R. A.; Hausinger, G.; Zeilinger, H.; Ramsteller, A.; Schmelz, H.; Knözinger, H. *Appl. Catal*. **1989**, *51*, 67.
(26) Rodenas, E.; Yamagouchi, T.; Hattori, H.; Tanabe, K. *J. Catal*. **1981**, *69*, 434.
(27) Stranick, M. A.; Houalla, M.; Hercules, D. M. *J. Catal*. **1987**, *106*, 362.
(28) Matralis, H. M.; Ciardelli, M.; Ruwet, M.; Grange, P. *J. Catal*. **1995**, *157*, 368.
(29) Reddy, B. M.; Kumar, M. V.; Reddy, E. P.; Mehdi, S. *Catal. Lett.* **1996**, *36*, 187.
(30) Gutierrez-Alejandro, A.; Gonzalez-Cruz, M.; Trombetta, M.; Busca, G.; Ramirez, J. *Microporous Mesoporous Mater*. **1998**, *23*, 265.
(31) Harlé, V.; Vrinat, M.; Scharff, J. P.; Durand, B.; Deloume, J. P. *Appl. Catal. A: General* **2000**, *196*, 261.
(32) Monaci, R.; Rombi, E.; Solinas, V.; Sorrentino, A.; Santacesaria, E.; Colon, G. *Appl. Catal. A: General* **2001**, *214*, 203.
(33) Reddy, B. M.; Ganesh, I.; Reddy, E. P. *J. Phys. Chem. B* **1997**, *101*, 1769.
(34) Church, J. S.; Cant, N. W.; Trimm, D. L. *Appl. Catal*. **1993**, *101*, 105.
(35) Ferrandon, M.; Björnbom, E. *J. Catal*. **2001**, *200*, 148.
(36) Beguin, B.; Garbowski, E.; Primet, M. *Appl. Catal*. **1991**, *75*, 119.
(37) Le Duc, C. A.; Campbell, J. M.; Rossin, J. A. *Ind. Eng. Chem. Res*. **1996**, *35*, 2473.
(38) Lane, G. S.; Kalenik, Z.; Wolf, E. E. *Appl. Catal*. **1989**, *53*, 183.
(39) Borchert, H.; Baerns, M. *J. Catal*. **1997**, *168*, 315.
(40) Kumar, K. N. P.; Keizer, K.; Burggraaf, A. J. *J. Mater. Chem*. **1993**, *3*, 1412.
(41) Trudinger, U.; Muller, G.; Unger, K. K. *J. Chromatogr*. **1990**, *35*, 111.
(42) Reddy, B. M.; Ganesh, I. *J. Mol. Catal. A: Chemical* **2001**, *169*, 207.
(43) Reddy, B. M.; Manohar, B.; Mehdi, S. *J. Solid State Chem*. **1992**, *96*, 233.
(44) Reddy, B. M.; Manohar, B.; Reddy, E. P. *Langmuir* **1993**, *9*, 1781.
(45) *Practical Surface Analysis*, 2nd ed.; Briggs, D., Seah, M. P., Eds.; Auger and X-Ray Photoelectron Spectroscopy, Wiley: New York, 1990; Vol. 1.
(46) Wagner, C. D.; Riggs, W. M.; Davis, L. E.; Moulder, J. F. In *Handbook of X-ray Photoelectron Spectroscopy*; Muilenberg, G. E., Ed.; Perkin-Elmer Corporation, Minnesota, 1978.
(47) Reddy, B. M.; Mehdi, S.; Reddy, E. P. *Catal. Lett*. **1993**, *20*, 317.
(48) Gopalan, R.; Lin, Y. S. *Ind. Eng. Chem. Res*. **1995**, *34*, 1189.
(49) Reddy, B. M.; Ganesh, I.; Reddy, E. P.; Fernández, A.; Smirniotis, P. G. *J. Phys. Chem. B* **2001**, *105*, 6227.
(50) Beattie, I. R.; Gilson, T. R. *Proc. R. Soc. London A* **1968**, *307*, 407.
(51) Beattie, I. R.; Gilson, T. R. *J. Chem. Soc. A* **1969**, 2322.
(52) Griffith, W. P.; Lesniak, P. J. B. *J. Chem Soc. A* **1969**, 1066.
(53) Knözinger, H.; Mestl, G. *Top. Catal*. **1999**, *8*, 45.
(54) Wachs, I. E. *Top. Catal*. **1999**, *8*, 57.
(55) Imamura, I.; Ishida, S.; Taramoto, H.; Saito, Y. *J. Chem. Soc., Faraday Trans*. **1993**, *89*, 757.
(56) Nag, N. K.; Massoth, F. E. *J. Catal*. **1990**, *124*, 127.
(57) Bukhtiyarov, V. I. *Catal. Today* **2000**, *56*, 403.
(58) Groenenboom, C. J.; Sawatzky, G.; Meijer, L.; Jellinek, F. *Organometall. Chem*. **1974**, *76*, C4.
(59) Barber, M.; Conner, J. A.; Derrick, L. M. R.; Hall, M. B.; Hillier, I. H. *J. Chem. Soc. Faraday Trans. 2* **1973**, *69*, 551.